

Brugada Syndrome and long QT syndrome can be caused by mutations in the gene encoding the Tbx5 transcription factor

P. Nieto-Marín, D. Tinaquero, R. García-Utrilla, T. Crespo, A. González-Guerra*, M. Rubio, R. Peinado‡, J.L. López-Sendón‡, J. Tamargo, J.A. Bernal*, J. Jalife*, R. Caballero, E. Delpón.

School of Medicine, Universidad Complutense de Madrid; *Centro Nacional de Investigaciones Cardiovasculares; ‡Cardiology Department, Hospital Universitario La Paz. Madrid, España

INTRODUCTION

Tbx5 is a transcription factor of the T-box family that plays a critical role in the cardiogenesis (1-3). It increases or represses the expression of different genes by binding to the consensus sequence (A/G)GGTGT(C/G/T)(A/G) within their minimal promoters (4). However, the transcriptional effect of Tbx5 also occurs in the adult heart. Indeed, it has been described that Tbx5 drives the expression of Nav1.5 channels in the adult mouse heart and plays a critical role in the control of the function of the cardiac conduction system (5). We hypothesized that mutations in Tbx5 could lead to cardiac arrhythmias with similar manifestations to those produced by mutations in the gene encoding Nav1.5 channels (*SCN5A*). Interestingly, the effects of Tbx5 on the cardiac sodium current (I_{Na}) generated by Nav1.5 channels are currently unknown. In the context of the ITACA Consortium (6-8), we identified two mutations in the *TBX5* gene encoding p.D111Y and p.F206L Tbx5, respectively. These mutations, that were predicted as pathogenic, were found in two probands diagnosed with long QT syndrome type 3 (LQT3) and Brugada syndrome (BrS), respectively. LQT3 and BrS are inherited arrhythmogenic syndromes associated with a high risk of sudden cardiac death and frequently caused by gain- and loss-of-function mutations, respectively, in the *SCN5A* gene encoding Nav1.5 channels (7-9). The main objective of the present work was to compare the effects of WT and mutant Tbx5 forms on the I_{Na} generated by Nav1.5 channels to unravel whether the mutations can underlie the LQT3 and the BrS of the carriers.

MATERIAL AND METHODS

- HL-1 cell culture and transfection (6,10,11):** HL-1 cells were cultured following procedures previously described and transiently transfected by using Lipofectamine 2000.
- Human induced Pluripotent Stem Cell derived cardiomyocytes (hiPSC-CMs) culture and infection (6,7):** hiPSC-CMs from Cellular Dynamics (iCell® Cardiomyocytes²) were thawed and cultured following manufacturer recommendations. Seven days after thawing, hiPSC-CMs were infected with lentiviral constructs coding WT, p.D111Y or p.F206L Tbx5.
- Transgenic mouse model (12):** Cardiac tissue-specific transgenic-like mice were generated by adeno-associated virus gene transfer. 6-week-old wild-type (WT) C57BL/6J mice were injected with viral genomes encoding GFP alone [Tbx5(-)] or fused to WT (Tbx5 WT), p.D111Y (Tbx5 p.D111Y) or p.F206L (Tbx5 p.F206L) Tbx5. Stable expression of WT and mutant Tbx5 proteins was reached after 6 weeks and maintained for at least five months as demonstrated by qPCR and WB. After 6 weeks, electrocardiographic and electrophysiological measurements were conducted.
- Patch Clamping (6-8,10,11,13):** In HL-1 cells, hiPSC-CMs, and enzymatically-isolated mouse ventricular myocytes the I_{Na} was recorded at room temperature using the whole-cell patch-clamp technique. In hiPSC-CMs and mouse ventricular myocytes, action potentials were recorded under the current-clamp configuration.
- Luciferase gene expression reporter assays and Western blotting (6-8,10,11,13):** Luciferase reporter assays were conducted in HL-1 cells transfected with pLightSwitch Prom luciferase vectors carrying the minimal promoter of human genes of interest or an empty vector. Western blots were performed in HL-1 cells transfected or not with WT or mutant Tbx5 or with shRNA against Tbx5 and incubated with each specific primary antibodies.

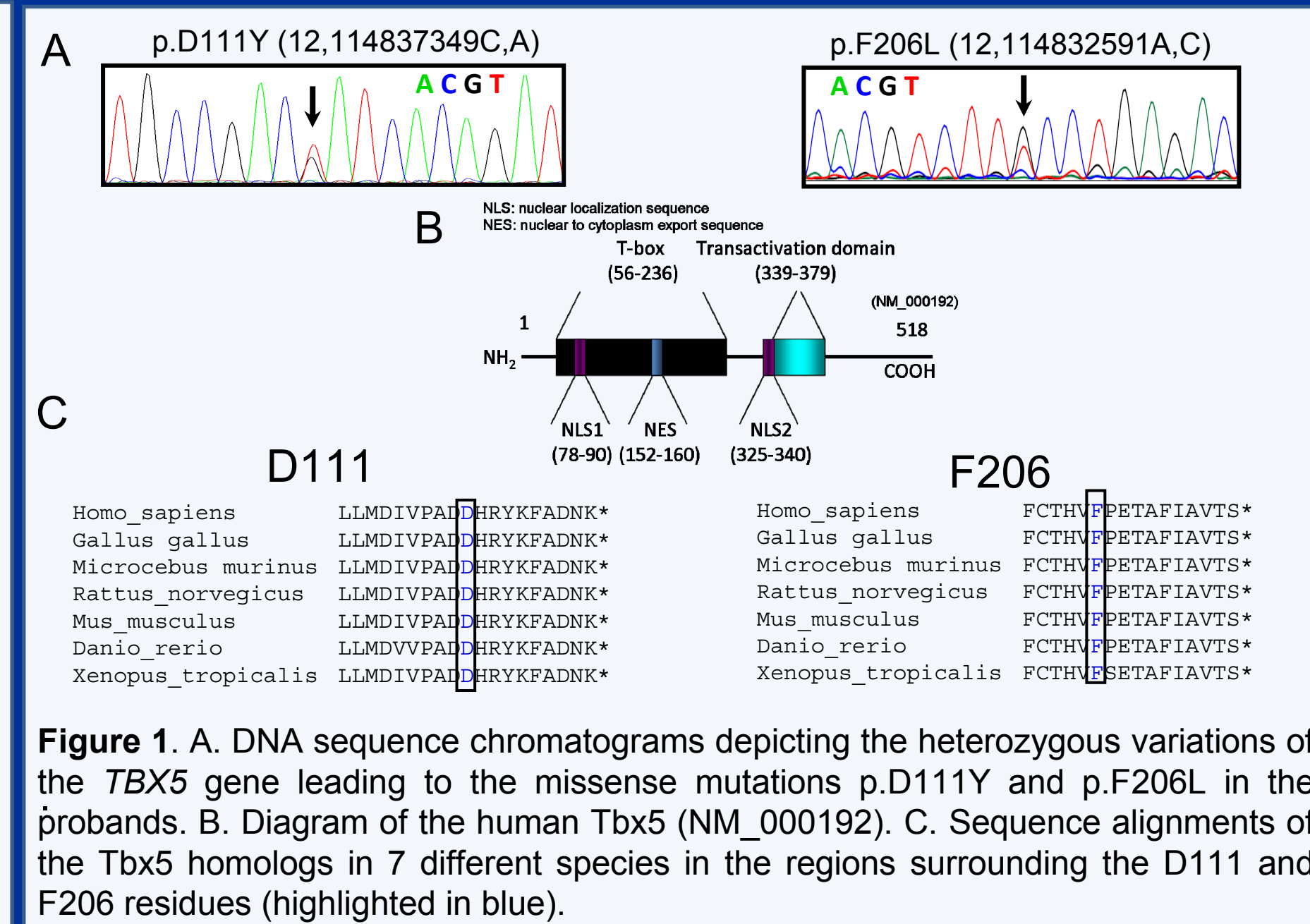


Figure 1. A. DNA sequence chromatograms depicting the heterozygous variations of the *TBX5* gene leading to the missense mutations p.D111Y and p.F206L in the probands. B. Diagram of the human Tbx5 (NM_001992). C. Sequence alignments of the Tbx5 homologs in 7 different species in the regions surrounding the D111 and F206 residues (highlighted in blue).

HL-1 CELLS

PEAK SODIUM CURRENT

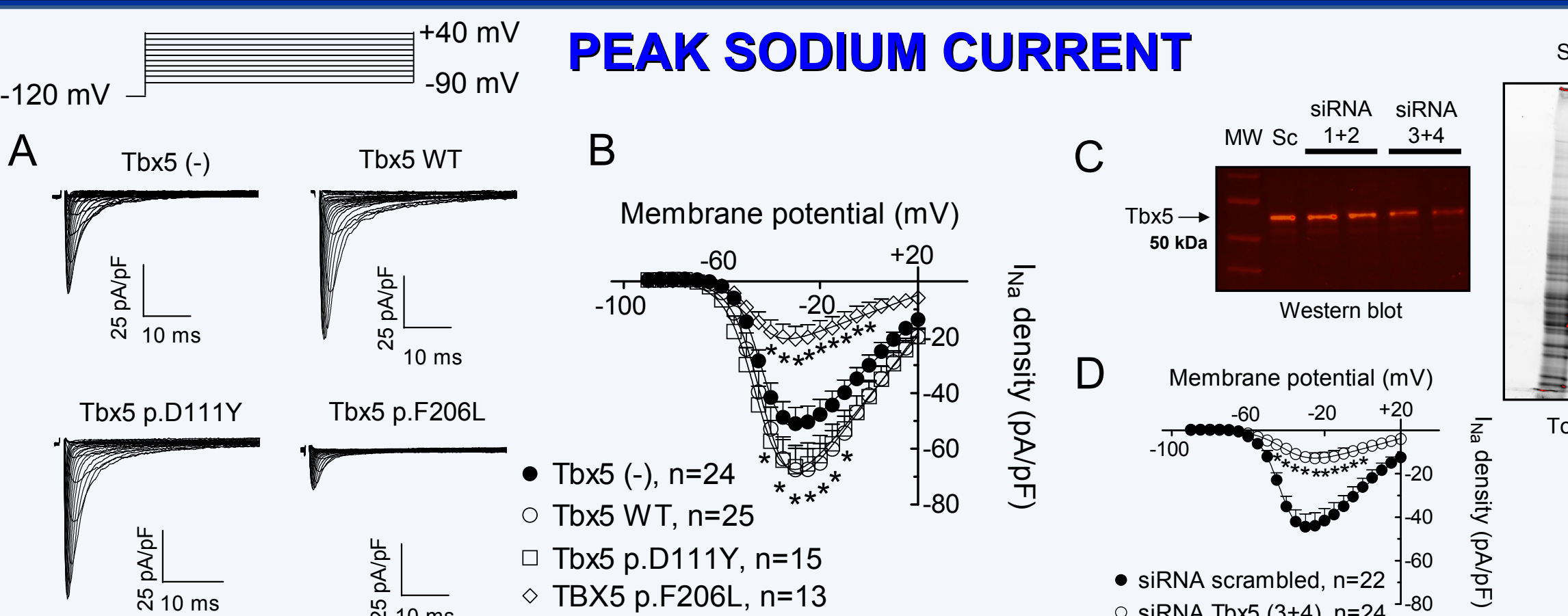


Figure 2. A. I_{Na} traces recorded by applying the protocol shown at the top in HL-1 cells transfected or not with WT, p.D111Y or p.F206L Tbx5. B. Mean current-density voltage curves for I_{Na} recorded in HL-1 cells transfected or not with the construct indicated. C. Representative Western blot showing the expression of Tbx5 (arrow) in HL-1 cells transfected or not with specific Tbx5 siRNAs duplexes or siRNA scrambled (Sc). The corresponding stain-free gel is depicted on the right to show the total protein. D. Mean current-density voltage curves for I_{Na} recorded in Tbx5-silenced HL-1 cells. In B and C, each point represents the mean±SEM of "n" experiments; * $P < 0.05$ vs Tbx5 (-).

TIME AND VOLTAGE DEPENDENCE

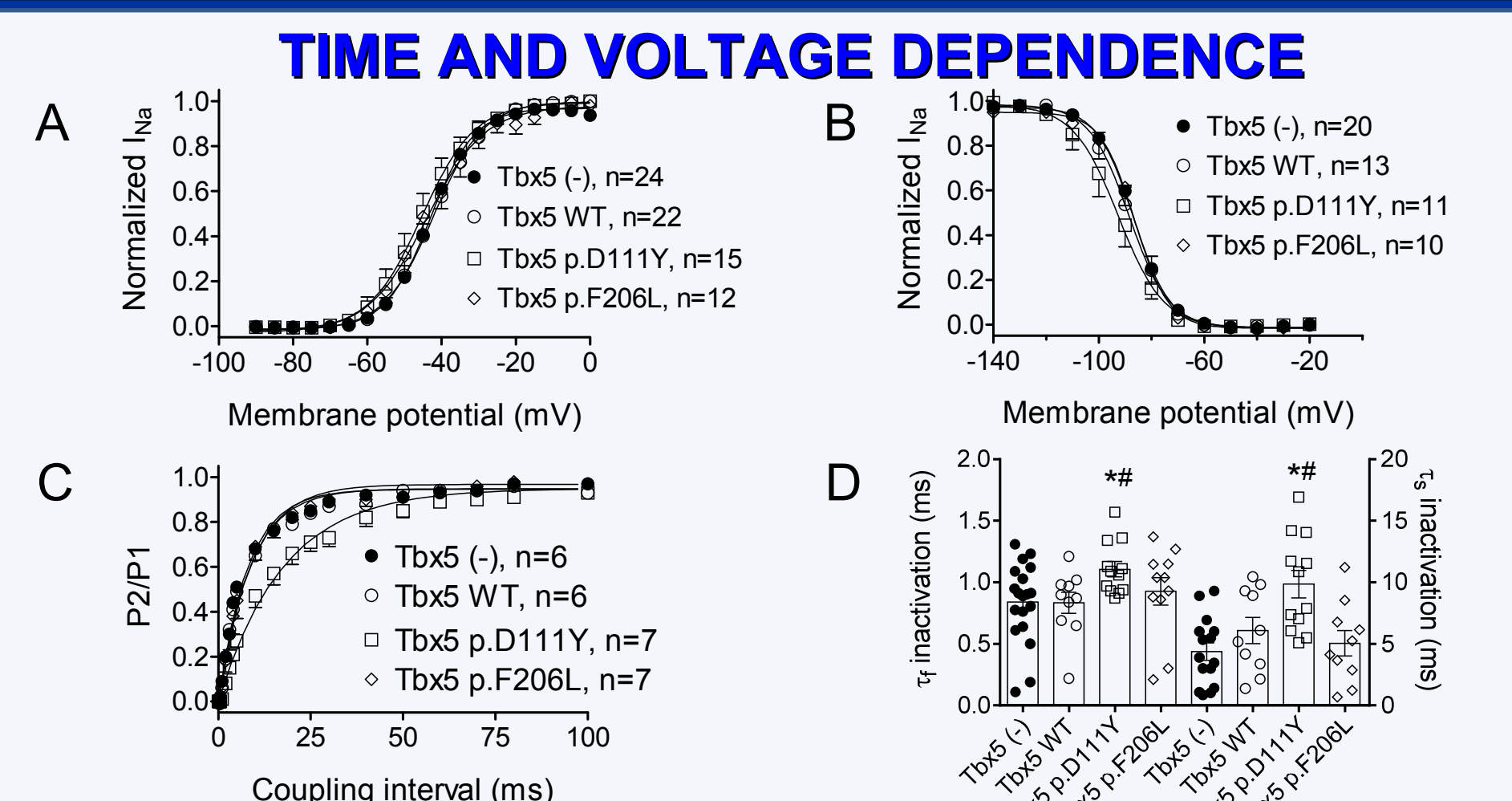


Figure 3. A-C. Conductance-voltage (A), inactivation (B), and reactivation (C) curves constructed for the I_{Na} recorded in HL-1 cells transfected or not with WT, p.D111Y or p.F206L Tbx5. D. Fast and slow time constants of inactivation obtained by fitting a biexponential function to the peak I_{Na} current traces. Each point/bar represents the mean±SEM of "n" experiments. * $P < 0.05$ vs Tbx5 (-) and # $P < 0.05$ vs Tbx5 WT.

LUCIFERASE ASSAYS AND WESTERN BLOTTING

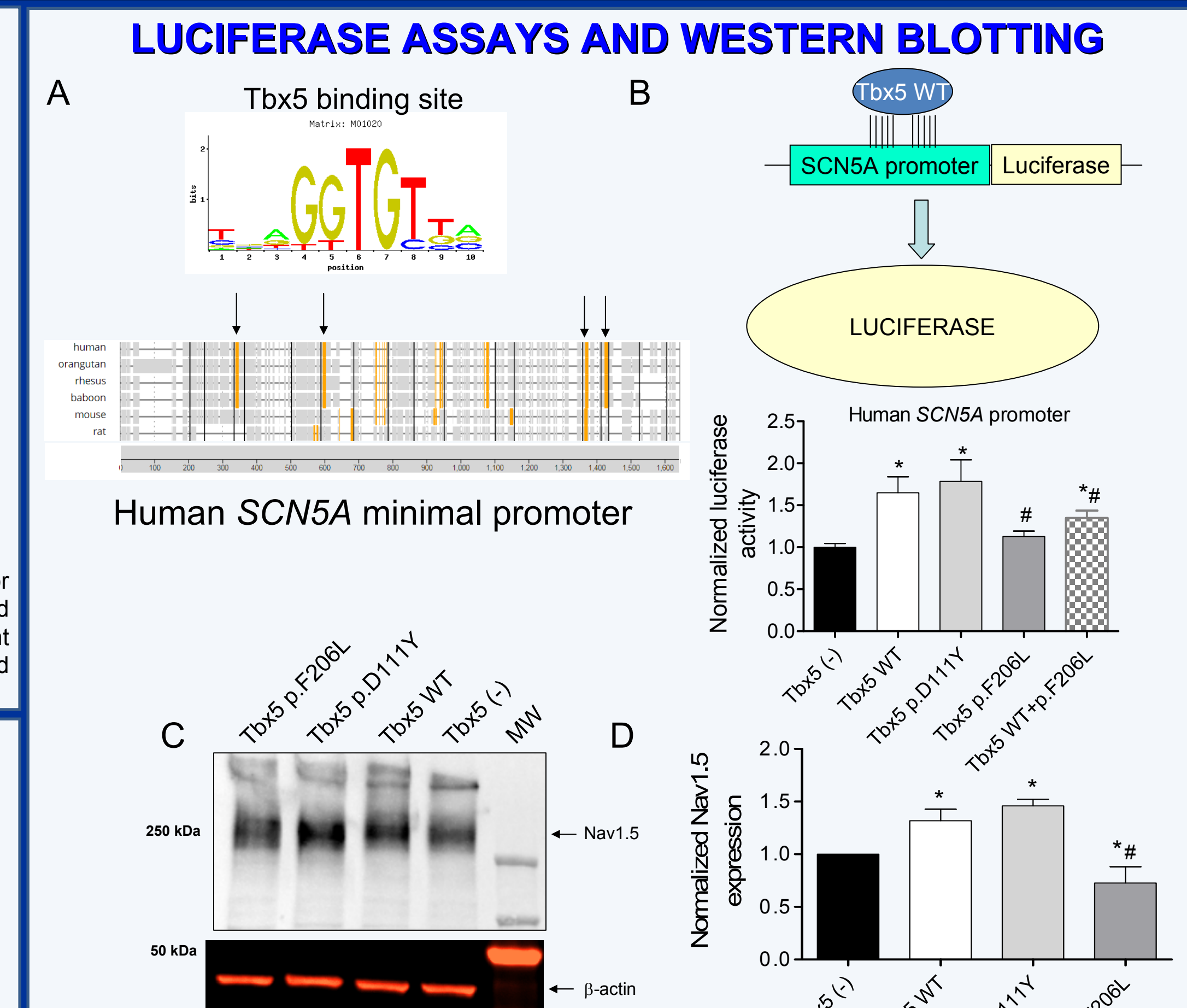


Figure 4. A. Results of the bioinformatic analysis performed to search the Tbx5-binding consensus sequence (top) within the human *SCN5A* minimal promoter by using the Contra V3 web tool. The most conserved Tbx5-binding sites predicted (orange) are marked with arrows. B. The upper part shows a schematic representation of the luciferase assay. The lower part shows the normalized luciferase activity measured in HL-1 cells transfected with the pLightSwitch_prom luciferase expression reporter vector carrying the *SCN5A* promoter together or not with Tbx5 WT, p.D111Y or p.F206L. C and D. Representative immunoblots (C) and densitometric analysis (D) after detection of Nav1.5 expression (arrow) in HL-1 cells transfected with the constructs indicated. β -actin was used as a loading control (bottom). Each bar is the mean±SEM of ≥ 4 experiments. In B and C, * $P < 0.05$ vs Tbx5 (-), # $P < 0.05$ vs Tbx5 WT.

LATE SODIUM CURRENT

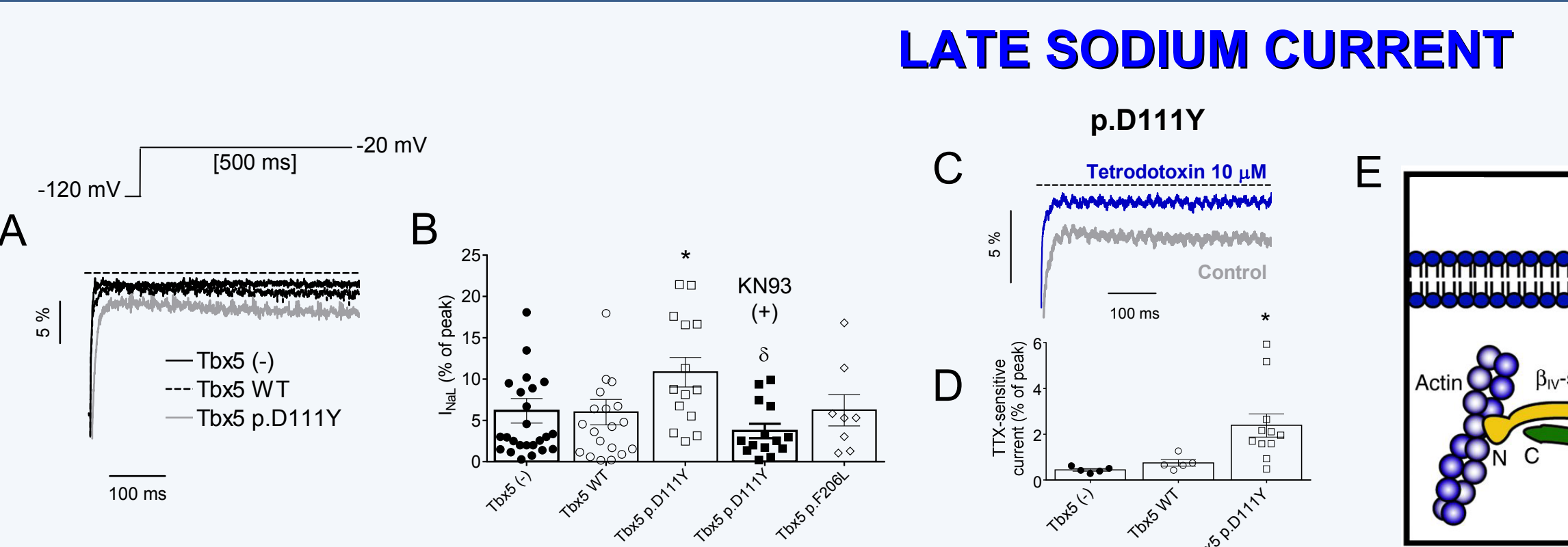


Figure 5. A. Normalized I_{Na} traces recorded by applying 500-ms pulses to -20 mV in HL-1 cells transfected or not with WT or p.D111Y Tbx5. B. Scatter dot plot and bar graph showing the I_{Na} amplitude measured as the percentage of the peak current recorded in HL-1 cells transfected with the constructs indicated. In a group of experiments, cells expressing the p.D111Y mutation were incubated with the CaMKII inhibitor KN93 (1 μ M) for 24 h. C. (Top) I_{Na} traces recorded in HL-1 cells expressing the p.D111Y mutation in the absence and presence of Tetrodotoxin (10 μ M). D. Scatter dot plot and bar graph showing the I_{Na} amplitude measured as the current sensitive to Tetrodotoxin in HL-1 cells transfected with the constructs indicated. E. Schematic diagram of the role of CaMKII and β -spectrin in the regulation of Nav1.5 channels and I_{Na} . F-G. Normalized luciferase activity measured in HL-1 cells transfected with the pLightSwitch_prom vector carrying the minimal promoters of human *CAMKII* (F) and *SNTBP4* (G) genes together or not with Tbx5 WT or p.D111Y. H-I. Western blot images of CaMKII and β -spectrin in HL-1 cells transfected with the constructs indicated. β -actin was used as a loading control (bottom). * $P < 0.05$ vs Tbx5 (-); # $P < 0.05$ vs Tbx5 WT; $\Delta P < 0.05$ vs Tbx5 p.D111Y.

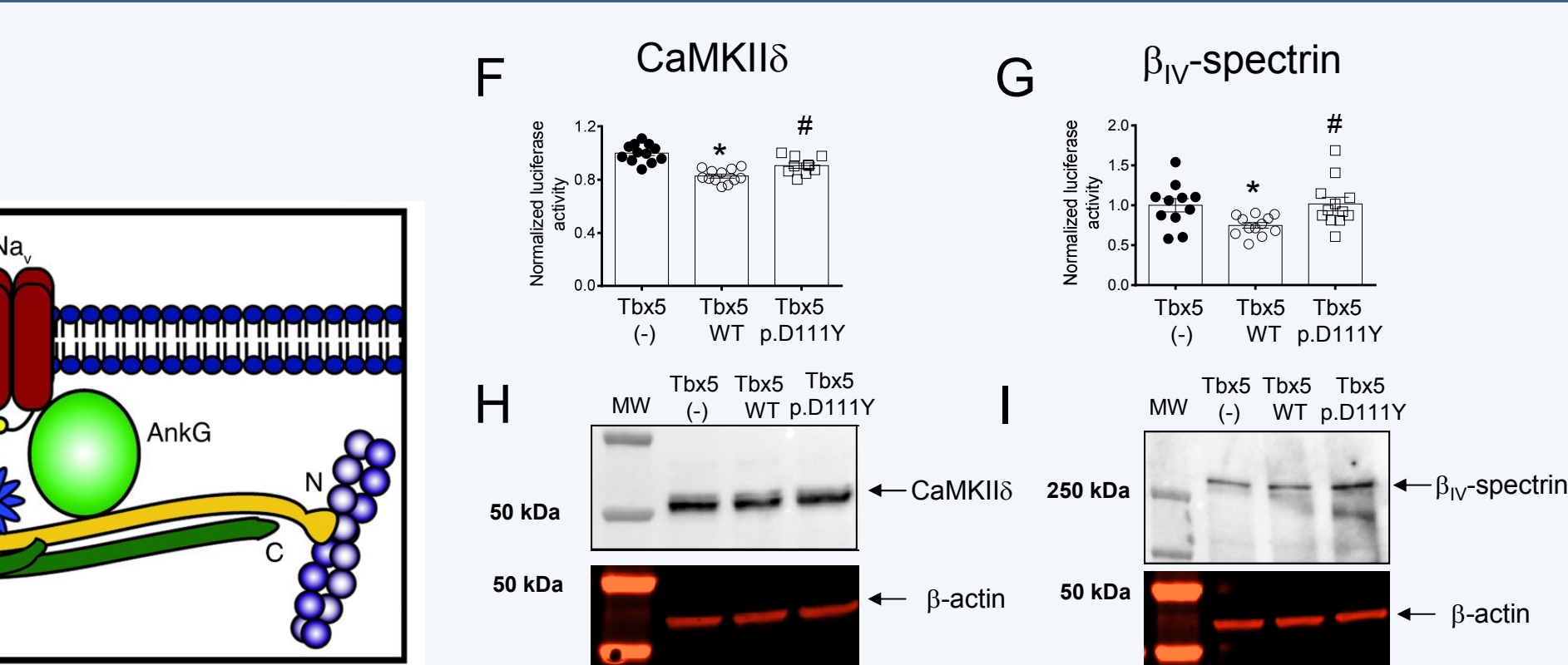


Figure 6. H-I. Western blot images of CaMKII and β -spectrin in HL-1 cells transfected with the constructs indicated. β -actin was used as a loading control (bottom). * $P < 0.05$ vs Tbx5 (-); # $P < 0.05$ vs Tbx5 WT; $\Delta P < 0.05$ vs Tbx5 p.D111Y.

hiPSC-CM

PEAK SODIUM CURRENT

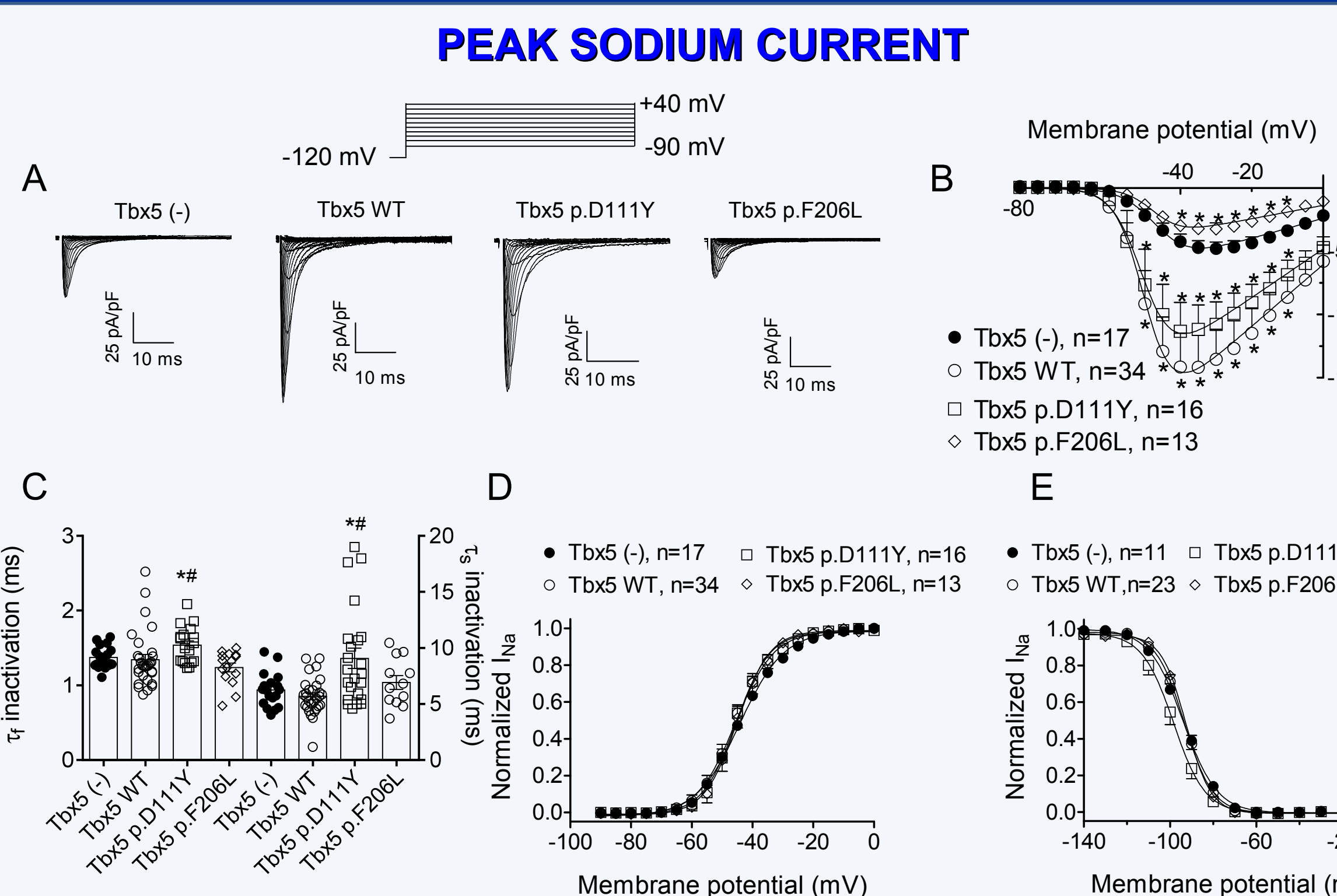


Figure 6. A-B. I_{Na} traces recorded by applying the protocol shown at the top (A) and mean current-density voltage curves (B) for I_{Na} recorded in hiPSC-CM infected or not with lentiviral vectors carrying the WT, p.D111Y or p.F206L Tbx5 constructs. C. Fast and slow time constants of inactivation obtained by fitting a biexponential function to the peak I_{Na} traces. D-E. Conductance-voltage (D) and inactivation (E) curves constructed for the I_{Na} recorded in hiPSC-CMs infected or not with the constructs indicated. Each point/bar represents the mean±SEM of "n" experiments. * $P < 0.05$ vs Tbx5 (-) and # $P < 0.05$ vs Tbx5 WT.

LATE SODIUM CURRENT

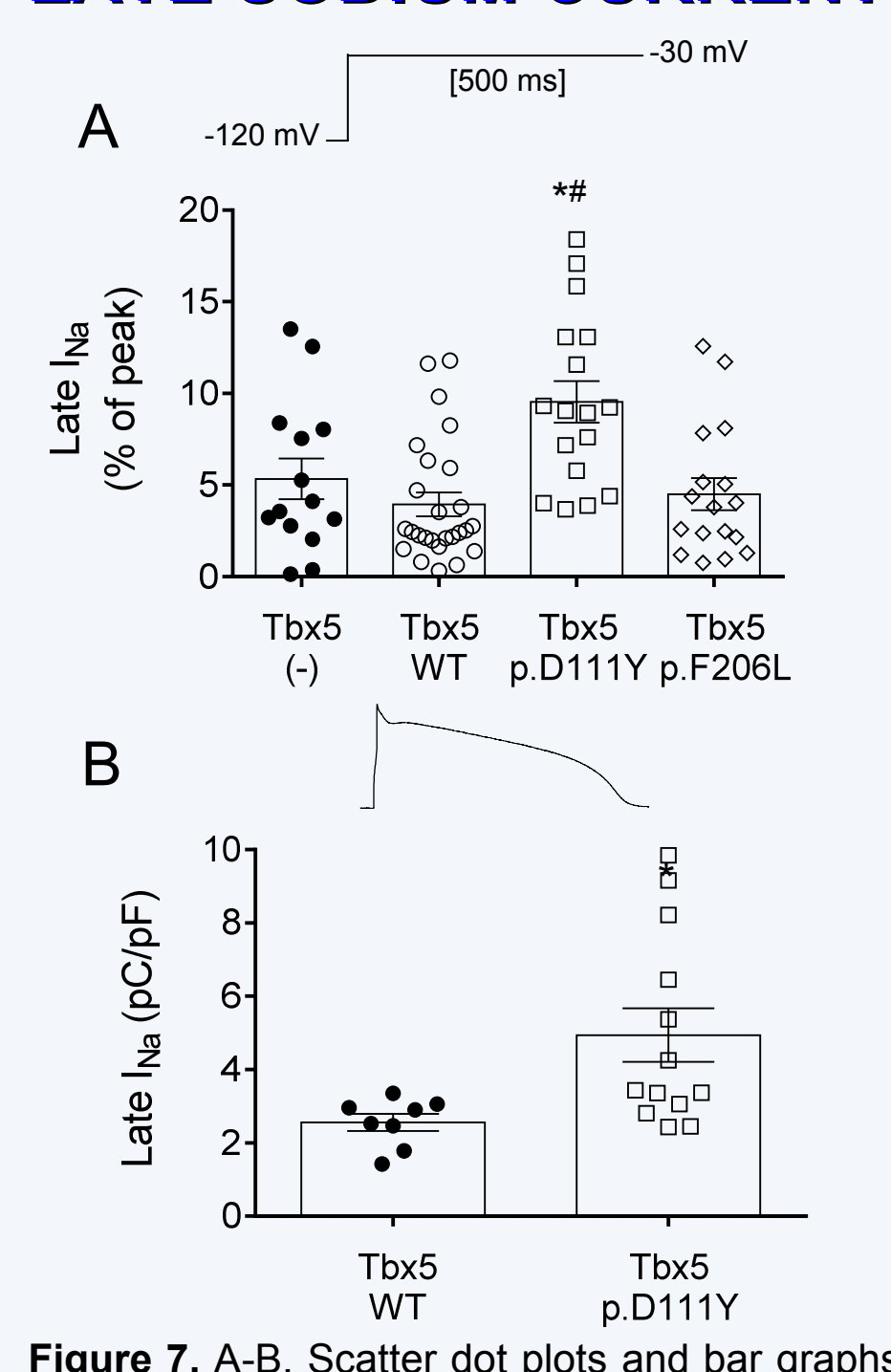


Figure 7. A-B. Scatter dot plots and bar graphs depicting the I_{Na} recorded by applying 500-ms pulses from -120 to -30 mV (A) or a human ventricular AP command signal (B) as voltage protocol in hiPSC-CMs infected with the constructs indicated. * $P < 0.05$ vs Tbx5 (-), # $P < 0.05$ vs Tbx5 WT.

TRANSGENIC MOUSE MODEL

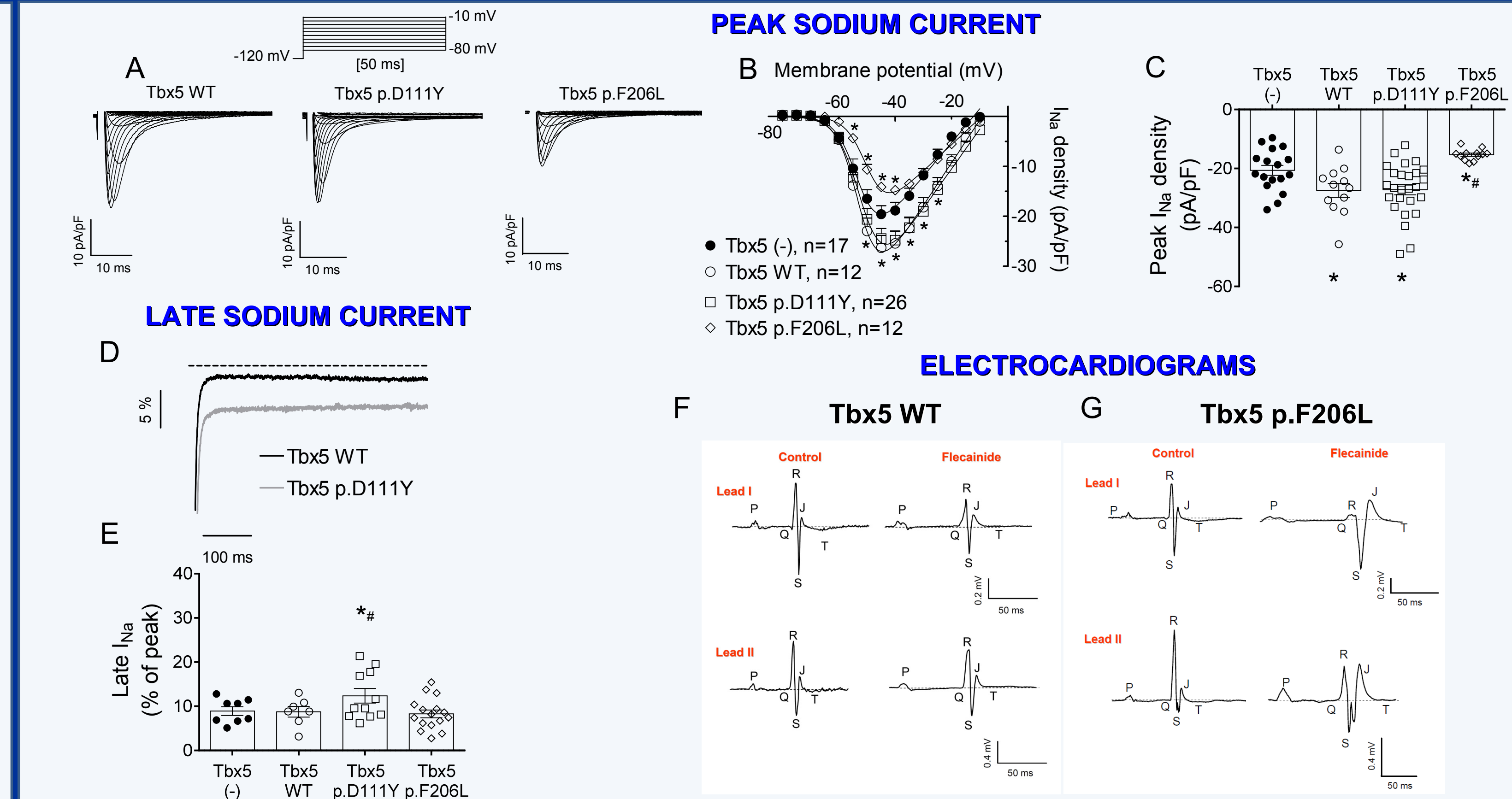


Figure 9. A-C. I_{Na} traces recorded by applying the protocol shown at the top (A), mean current-density voltage curves (B) and peak current density (C) for I_{Na} recorded in ventricular myocytes isolated from cardiac-specific transgenic like mice expressing AAV coding or not WT, p.D111Y or p.F206L Tbx5. D. Normalized I_{Na} traces recorded by applying 500-ms pulses from -120 to -40 mV in mouse ventricular myocytes isolated from WT and p.D111Y mice. E. Scatter dot plots and bar graphs showing I_{Na} amplitude measured as the percentage of peak current recorded in ventricular myocytes from the mice indicated. F-G. ECG recordings (Leads I and II) conducted *in vivo* in anesthetized WT (F) or p.F206L (G) Tbx5 mice in the absence or presence of Flecainide (20 mg/kg). * $P < 0.05$ vs Tbx5 (-) and # $P < 0.05$ vs Tbx5 WT.

ACTION POTENTIALS

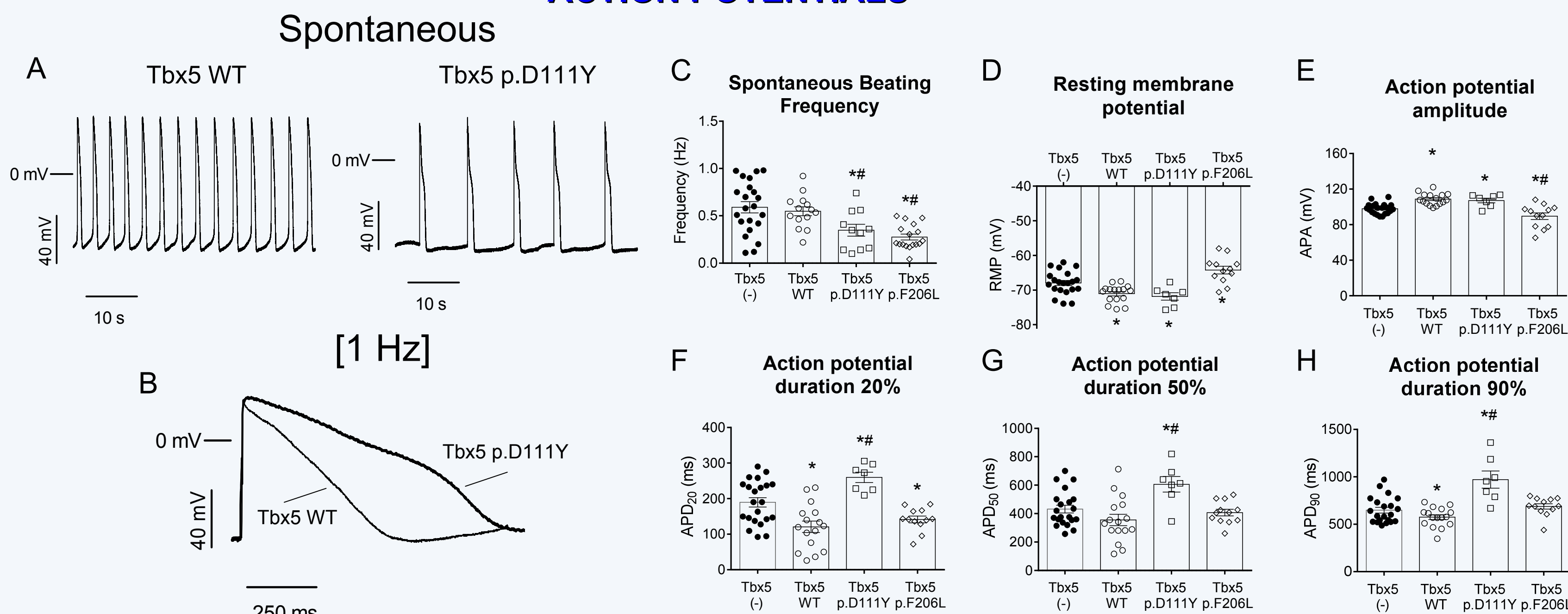


Figure 8. A-B. Representative action potentials recorded in hiPSC-CMs infected or not with lentiviral constructs coding WT or p.D111Y Tbx5 generated spontaneously (A) or by driving the cells at a frequency of 1 Hz (B). C-H. Scatter dot plots and bar graphs depicting mean spontaneous beating frequency (C), resting membrane potential (D), action potential amplitude (E), and action potential duration measured at 20% (F), 50% (G) and 90% (H) of repolarization for action potentials recorded in hiPSC-CMs infected with the constructs indicated. * $P < 0.05$ vs Tbx5 (-); # $P < 0.05$ vs Tbx5 WT.

CONCLUSIONS

- WT and p.D111Y Tbx5 significantly increased the peak I_{Na} density in HL-1, hiPSC-CMs, and mouse ventricular myocytes, as a consequence of their pro-transcriptional effect over the *SCN5A* gene.
- The p.F206L mutation prevented the Tbx5-protranscriptional effect over the *SCN5A* gene, markedly decreasing the peak I_{Na} and the amplitude of the action potentials recorded in hiPSC-CMs. These effects account for the BrS of the carriers.
- The p.D111Y mutation abolished the Tbx5-repressor activity over the *CAMKII* and *SNTBP4* genes, increasing the expression of CaMKII δ and β -spectrin and, therefore, the I_{Na} .
- As a result of their effects on the I_{Na} , p.D111Y significantly lengthened the duration of the action potentials recorded in hiPSC-CMs. This effect accounts for the LQT3 of the mutant carriers.

ACKNOWLEDGMENTS AND FUNDING

We thank Sandra Sacristán and Paloma Vaquero for their invaluable technical assistance. This work was supported by grants from Ministerio de Ciencia, Innovación y Universidades (SAF2017-88116-P), Comunidad Autónoma de Madrid (S2017/BMD-3738), Instituto de Salud Carlos III (P16/00398), Spanish Society of Cardiology, and Fondos FEDER.

REFERENCES

- Gruelich F et al. Cardiovascular Research 2011; 91: 212-22.
- Al-Qattan MM et al. Gene. 2015; 560:129-36.
- Stirnimann CU et al. J Mol Biol. 2010; 400:71-81.
- Ghosh TK et al. Hum Mol Genetics. 2001; 10:1983-94.
- Arnolds DE et al. J Clin Invest. 2012; 122:2509-18.
- Caballero R et al. Proc Natl Acad Sci USA. 2017; 114: E416-E425.
- Nieto-Marín P. Rev Esp Cardiol. 2019; 72:324-32.
- Antzelevitch C & Patocskaï B. Curr Probl Cardiol. 2016; 41:7-57.
- Pérez-Hernández M et al. Cardiovasc Res. 2016; 109:431-41.
- Matamoros M et al. Cardiovasc Res. 2016; 110:279-90.
- Cruz FM et al. J Am Coll Cardiol. 2015; 65:1438-50.
- Utrilla RG et al. Front Physiol. 2017; 8:903.